Supplementary Information

Resting-state functional network correlates of psychotic symptoms in schizophrenia

Anna Rotarska-Jagiela[a,b,c] , Vincent van de Ven[d], Viola Oertel-Knöchel[c], Peter J. Uhlhaas[a,c], Kai Vogeley[b], David E.J. Linden[e]

[a] Max Planck Institute for Brain Research, Department of Neurophysiology, Deutschordenstr. 46, 60528 Frankfurt a.M., Germany

[b] University of Cologne, Department of Psychiatry and Psychotherapy, Kerpenerstr. 62, 50924 Cologne, Germany

[c] Johann Wolfgang Goethe University, Department of Psychiatry, Neurophysiology and Neuroimaging Lab and Brain Imaging Center, Heinrich-Hoffmann-Str. 10, 60528 Frankfurt/Main, Germany

[d] Maastricht University, Department of Cognitive Neuroscience, PO Box 616, 6200 MD, Maastricht, The Netherlands

[e] Bangor University, School of Psychology and North Wales Clinical School, Adeilad Brigantia, Penrallt Road, Gwynedd LL57 2AS, United Kingdom

Supplementary Methods: Number of components

The choice of number of components is a complicated issue in ICA analyses. As Calhoun et al. (2009) state in their review, the number of components remains a free parameter in spatial ICA of fMRI data. There are currently several algorithms that provide some 'optimal' number of components, but these numbers are very dependent on the kind of algorithm used and how functional data are prepared (c.f., Calhoun et al. 2001; Beckmann and Smith 2005; Cordes and Nandy 2005). Moreover, all currently existing algorithms base their estimate on PCA decompositions (i.e., pre-whitened data), whereas ICA components are ultimately estimated using a statistical independence criterion. Thus, it is very likely that the algorithms may miss-specify the optimal dimensionality for ICA. Finally, the analytical penalty for estimating too many components (over-estimation) is relatively limited and can be controlled by examining the correlations between the component time courses: If over-estimation results in splitting of a source into multiple components, the component time courses should be highly correlated. Conversely, with under-estimation, information is simply discarded from the analysis and cannot be retrieved. Several authors (Formisano et al. 2004; McKeown et al. 1998) provide intuitive examples of cases in which full dimensionality (i.e., number of components equals number of measured volumes) revealed spatiotemporal dynamics that were not found with lower dimensionalities. Therefore, the existing algorithms by no means provide definitive estimations of ICA dimensionality.

In our study, we chose to decompose the data into 45 spatial components. We initially explored the estimation of number of components for individual data using AIC and minimum description length (MDL) (Calhoun et al., 2001), and we obtained a mean estimate of 35 components across all datasets. However, this resulted in very noisy decompositions in which components that are very reliably reported in the literature, such as DMN, were not present in a portion of the data. Thus, we considered that for our data 35 components provided too

strong an under-fitting problem. At 45 components we found higher spatial correlation between components within selected clusters for the healthy control group, which provides a reliability estimate for the selected components. The decomposition with 45 components was also superior in terms of spatial correlations when compared to the decomposition with 50 components. Our initial estimate for the optimal number of components thus resulted in underfitting (loss of relevant information), and choosing even higher number of components in overfitting, which was remediated in the solution with 45 components. This number fits within the range of components that are used in the literature, which varies between 20 and 60 components.

Supplementary Methods: Calculation of goodness-of-fit indices

For this analysis, we calculated spatial goodness-of-fit (GOF) indices (Greicius et al., 2004; Esposito et al., 2008), which were quantified as the spatial correlation of a functional connectivity map to an independent spatial template. For each of the five networks, the independent template was calculated as the 'leave-one-out' mean of the connectivity maps, i.e., the mean calculated of all connectivity maps in a set except for the connectivity map for which the GOF is calculated. The GOF correlation values (r values) were normalized using Fisher's Z-transformation,

$$Z_{Fisher} = ½*\ln((1+r)/(1-r))$$

and were tested for group differences using a multivariate regression analysis with group as fixed factor and the GOFs of the five networks as dependent variables.

Supplementary Methods: Laterality indices

Laterality indices (LIs) were computed from the regression connectivity maps by

$$LI=(L-R)/(L+R)$$

Where L (R) refers to the number of voxels surpassing a connectivity threshold (1 SD) in the left (right) hemisphere. An LI of 1 (-1) refers to complete left-sided (right-sided) laterality of the connectivity map.

Supplementary Tables

Table S1. Mean coordinates of target areas in the five spatial templates. LH (RH), left (right) hemisphere; BA, Brodmann area; STG, superior temporal gyrus (includes BA 41, 42, 22, 43 and 13); PTP, posterior temporal plane (includes BA 22, 39, 40). Region size is reported in mm3.

	Talairach coordinates				
template	x	y	z	size	area
DMN	-3	-49	22	17793	LH BA 23
rFPN	33	-59	41	10179	RH BA 7
lFPN	-45	-55	39	12177	LH BA 7
AC	-44	-23	7	10638	LH STG
	44	-15	8	9720	RH STG
lFT	-56	-43	14	10530	LH PTP
	-51	16	13	9099	LH BA 44

Table S2. Regions of the five functional connectivity networks. Regions are described by size (mm3) and Talairach coordinates (center of mass). Random-effects (RFX) results are listed as one-sample T-values of all subjects (df=31, ignoring group membership). Between-group effects are listed as two-sample T-values (df=30), and were only calculated for voxel regions that passed the cluster threshold estimated from the data (k, in mm3). FCN, functional connectivity network; DMN, default-mode network; rFPN, right fronto-parietal network; lFT, left fronto-temporal network; AC, auditory network; lFPN, left front-parietal network.

						RFX		between-groups	
FCN	k	size	x	y	z	T	P	T	P
DMN	3051	3915	59	-2	-12	6.4	4.0e-07	-0.2	0.847
		11664	44	-59	27	10.5	1.0e-11	0.4	0.6894
		486	-1	-11	9	5.2	1.0e-05		
		51462	-4	-59	27	21.1	6.0e-20	2.3	0.0264
		58671	-1	43	0	10.0	4.0e-11	-0.5	0.5995
		1350	-22	-20	-9	5.0	2.0e-05		
		378	-34	4	48	3.5	0.001		
		14931	-46	-59	21	9.5	1.0e-10	-0.8	0.4167
		6102	-55	-8	-12	8.6	9.0e-10	0.3	0.7811
rFPN	1539	189	56	-32	-12	4.0	0.0004		
		28836	44	-53	36	11.3	2.0e-12	0.1	0.9523
		52758	32	52	15	10.8	4.0e-12	2.5	0.017
		864	2	-92	18	4.2	0.0002		

		432	2	-77	-18	3.8	0.0006		
		1404	-40	52	12	5.1	1.0e-05		
		162	-55	16	36	3.2	0.003		
		2430	-40	-62	42	4.2	0.0002	-3.3	0.0027
		1134	-61	-41	-9	4.8	3.0e-05		
lFT	1701	243	59	-47	15	3.3	0.003		
		3456	56	-35	0	4.4	0.0001	0.7	0.5062
		10935	56	22	6	5.9	1.0e-06	-0.1	0.9056
		432	32	-74	-18	3.7	0.0007		
		486	2	-92	24	4.3	0.0002		
		891	14	-86	-12	3.5	0.001		
		189	-4	-20	9	3.7	0.0008		
		324	-4	58	0	4.5	9.0e-05		
		243	-1	-41	-3	3.9	0.0005		
		44766	2	55	30	10.0	3.0e-11	0.8	0.4029
		43470	-52	28	0	8.0	5.0e-09	-0.3	0.7548
AC	1323	44226	56	-8	12	10.4	1.0e-11	-0.9	0.3932
		729	35	-41	60	4.3	0.0002		
		486	20	-2	-6	4.1	0.0002		
		459	-1	-38	0	4.0	0.0004		
		4671	2	4	39	6.2	6.0e-07	-0.8	0.4074
		1566	-1	-89	27	6.3	5.0e-07	-1.4	0.1597
		1377	-1	-50	57	5.1	2.0e-05	-2.0	0.0503
		270	-22	1	-6	3.7	0.0008		
		216	-55	-62	6	3.8	0.0007		
		34209	-61	-23	18	8.8	6.0e-10	0.1	0.9123
lFPN	1350	243	53	-47	-15	4.2	0.0002		
		270	-4	-38	-3	3.8	0.0007		
		405	-49	-47	-9	3.9	0.0005		
		97470	-25	-74	36	8.5	1.0e-09	1.1	0.2915

Supplementary Figures

Figure S1. Spatial group maps of the five networks. A-E: One-sample T-maps of regression functional connectivity maps of all participants are superimposed on transverse anatomical images (averaged across all participants). F-J: SogICA group maps are one-sample T-maps of spatial ICA components that are grouped into clusters of spatially homogenous components (Esposito et al., 2005; van de Ven et al., 2008). T-maps of regression and sogICA were thresholded at a false-positive rate of q=0.01. Left hemisphere is depicted on the left of each image. A,F: Default-mode network (DMN). B,G: right fronto-parietal network (rFPN). C,H: left fronto-temporal network (lFT). D,I: Auditory cortex network (AC). E,J: left fronto-parietal network (lFPN).

Figure S2. Scatterplots of regression-based (abscissa) and sogICA-based (ordinate) functional connectivity estimates for the five selected networks. Data points are of one-sample T-maps of individual connectivity maps of each network (see Figures 1 and S1). Correlation for each comparison is reported above each scatterplot. Minimum correlation of 0.75 indicates a very strong similarity between the two types of functional connectivity estimates.

Supplementary References

Beckmann, C.F., and Smith, S.M. Tensorial extensions of independent component analysis for multisubject fMRI analysis. Neuroimage:294-311, 2005.

Calhoun, V.D.; Adali, T.; Pearlson, G.D.; and Pekar, J.J. Spatial and temporal independent component analysis of functional MRI data containing a pair of task-related waveforms. Hum Brain Mapp, 13(1):43-53, 2001.

Calhoun, V.D.; Liu, J.; and Adali, T. A review of group ICA for fMRI data and ICA for joint inference of imaging, genetic, and ERP data. Neuroimage, 45(1 Suppl):S163-72, 2009.

Cordes, D., and Nandy, R.R. Estimation of the intrinsic dimensionality of fMRI data. Neuroimage, 29:145-154, 2005.

Esposito, F., Scarabino, T., Hyvarinen, A., Himberg, J., Formisano, E., Comani, S., Tedeschi, G., Goebel, R., Seifritz, E., and Di Salle, F. (2005). Independent component analysis of fMRI group studies by self-organizing clustering. Neuroimage 25, 193-205.

Esposito F, Aragri A, Pesaresi I, Cirillo S, Tedeschi G, Marciano E, Goebel R, Di Salle F: Independent component model of the default-mode brain function: combining individual-level and population-level analyses in resting-state fMRI. Magn Reson Imaging 2008; 26(7):905-13.

Formisano, E.; Esposito, F.; Di Salle, F.; and Goebel, R. Cortex-based independent component analysis. Magnetic Resonance Imaging, 22:1493-1504, 2004.

Greicius MD, Srivastava G, Reiss AL, Menon V: Default-mode network activity distinguishes Alzheimer's disease from healthy aging: evidence from functional MRI. Proc Natl Acad Sci U S A 2004; 101(13):4637-42.

McKeown, M.J.; Makeig, S.; Brown, G.G.; Jung, T.P.; Kindermann, S.S.; Bell, A.J.; and Sejnowski, T.J. Analysis of fMRI data by blind separation into independent spatial components. Hum Brain Mapp, 6(3):160-88, 1998.

van de Ven, V., Bledowski, C., Prvulovic, D., Goebel, R., Formisano, E., Di Salle, F., Linden, D. E., and Esposito, F. (2008). Visual target modulation of functional connectivity networks revealed by self-organizing group ICA. Hum Brain Mapp 29, 1450-1461.

Figure S1

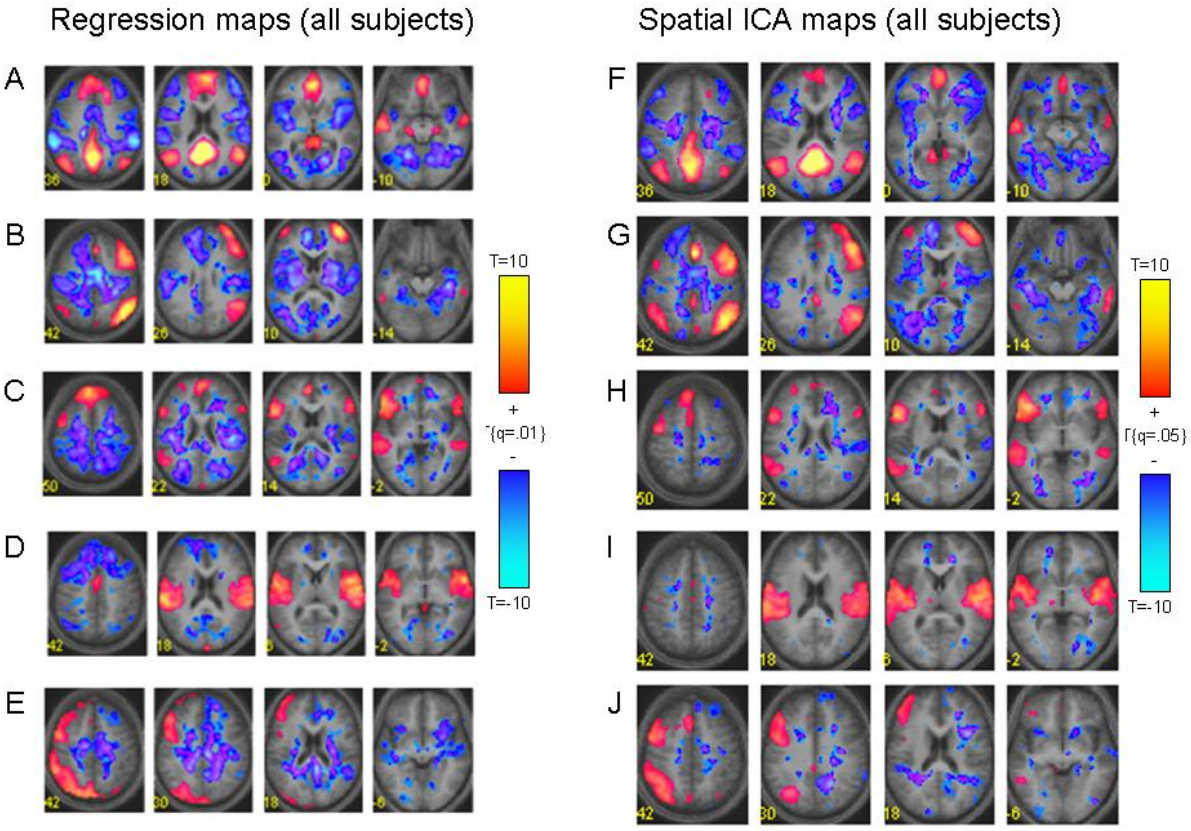
Regression maps (all subjects)
Spatial ICA maps (all subjects)
A
B
C
D
E
F
G
H
I
J
T=10
+
˜{q=.01}
-
T=-10
T=10
+
Γ{q=.05}
-
T=-10

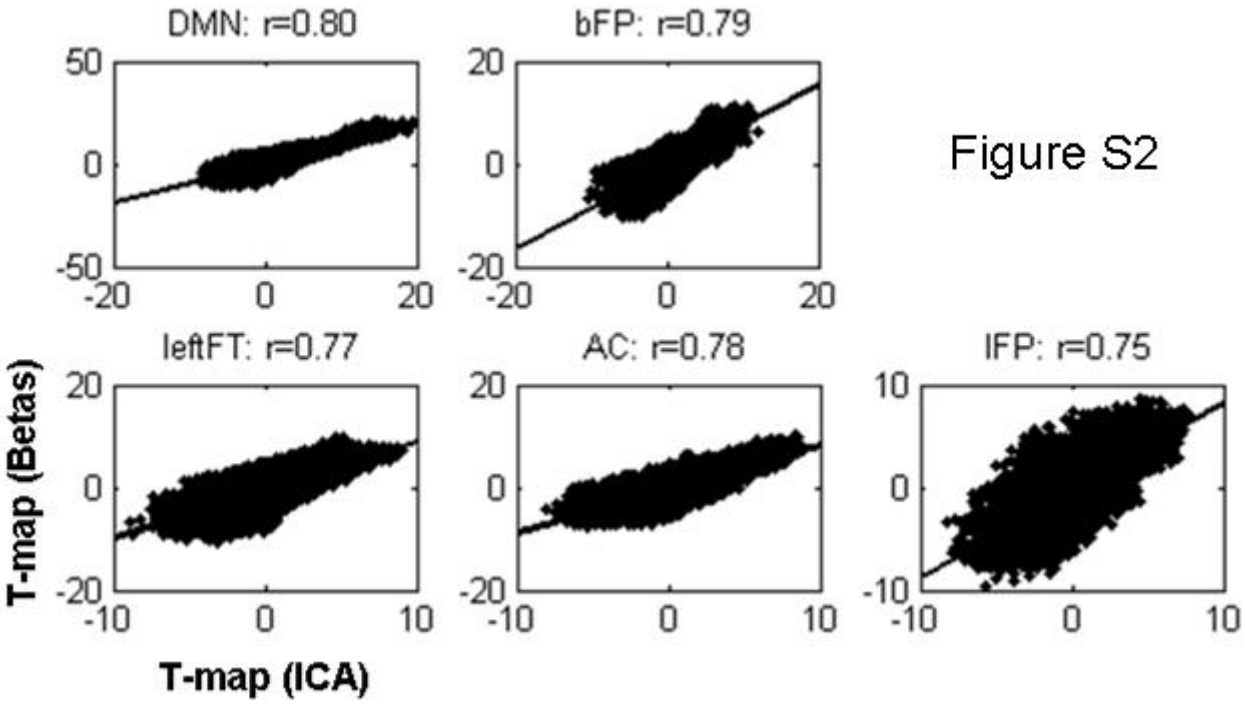
DMN: r=0.80
bFP: r=0.79
leftFT: r=0.77
AC: r=0.78
lFP: r=0.75
T-map (Betas)
T-map (ICA)

Figure S2